Carbocations from dibenz[*a,j*]anthracene and dibenz[*a,h*]anthracene, their methylated derivatives, and oxidized metabolites; a stable ion and DFT study

Takao Okazaki,[a] Joong-Hyun Chun, and Kenneth K. Laali*

Department of Chemistry, Kent State University, Kent, OH 44242, USA
[a] Present address: Department of Chemistry for Materials, Mie University, Tsu 514-8507 Japan
E-mail: klaali@kent.edu

Contribution for the commemorative issue in honor of Prof. Ted Sorensen

Abstract

Parent dibenz[*a,j*]anthracene DB[*a,j*]A **1** is protonated (in TfOH/SO_2ClF) to give a 1:1 mixture of *meso*-protonated arenium ions **1aH**$^+$ and **1bH**$^+$. The 7-methyl- DB[*a,j*]A **2** is protonated (in FSO_3H/SO_2ClF or TfOH/SO_2ClF) at the unsubstituted *meso* position (C-14) to give **2H**$^+$, and the 7,14-dimethyl derivative **3** is *ipso*-protonated (in FSO_3H/SO_2ClF) at C-14 to give **3H**$^+$. Experimental and/or GIAO-NMR derived $\Delta\delta^{13}C$ values, as well as changes in the computed NPA charges, were used to derive charge delocalization maps for the protonated carbocations derived from parent and methylated DB[*a,j*]A and DB[*a,h*]A. DFT and GIAO-DFT were also employed to model the bay-region *anti*-diol-epoxides (DEs), their derived carbocations, and model covalent adducts. The higher tumorigenic potenties of DB[*a,h*]A and its methylated derivatives as compared to those of DB[*a,j*]A are reflected in relative ease of carbocation formation from the DEs. Preference for *anti* stereochemistry in the covalent adducts derived from DB[*a,h*]A increases with increasing steric crowding at the bay-region.

Keywords: Dibenz[*a,j*]anthracene, dibenz[*a,h*]anthracene, carbocations via protonation, bay-region carbocations, charge delocalization mapping, DFT and GIAO-DFT

Introduction

Polycyclic aromatic hydrocarbons (PAHs) are widespread environmental contaminants that are metabolically activated to form dihydrodiols, that upon further epoxidation, generate diol-epoxides (DEs) as ultimate carcinogens.[1-4] Reactive diol-epoxides could rapidly intercalate into DNA to form non-covalent complexes, from which benzylic carbocations could form in an acid-

catalyzed ring opening step.[5,6] The resulting delocalized carbocations are capable of forming covalent adducts with the nucleotides on DNA and RNA. The PAHs that possess bay- and fjord-region(s) are especially potent DNA alkylating agents, and numerous studies have underscored the importance of benzylic carbocations as intermediates in the metabolism of bay- and fjord-region PAHs.[7]

Extensive structure-activity relationship data exist for the benz[*a*]anthracene (BA) skeleton,[8] and stable ion studies have also been carried out to model the carbocations derived from various substituted BAs.[9,10] In comparison, limited comparative bioactivity data are available for isomeric dibenzanthracenes (DBAs), namely DB[*a,j*]A, DB[*a,h*]A and DB[*a,c*]A (Fig 1), and their methylated derivatives.[8]

DB[*a,j*]A is less tumorigenic than DB[*a,h*]A.[8a] It is epoxidized in mammalian liver systems at C-3/C-4 (M-region) as a minor metabolite which is enzymatically hydrated to 3,4-*trans*-dihydrodiol and further epoxidized to 3,4-diol-1,2-epoxide (see also Fig 2).[11] The *trans*-DE enantiomers were shown to form covalent adducts with DNA.[12]

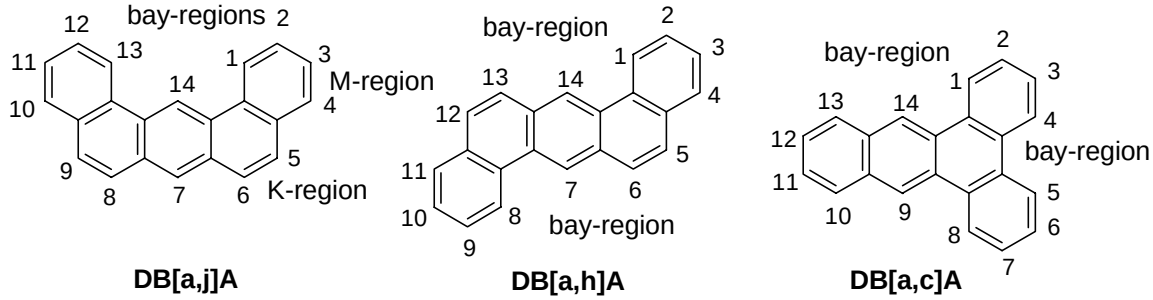

Figure 1. Isomeric DBA's.

Formation of the 5,6-dihydrodiol (K-region) has also been reported in the metabolism of DB[*a,j*]A, as well as other more polar metabolites which were attributed to the bis-dihydrodiols.[13] The 3,4-dihydrodiol is the major metabolite of DB[*a,h*]A, with the 1,2-dihydrodiol identified as the minor metabolite. The 3,4-dihydrodiol was found be highly tumorigenic (see also Fig 2).[13] The bay-region DE derived from DB[*a,h*]A formed covalent adducts with DNA.[14] The 7-nitro-DB[*a,h*]A, with a buttressed nitro group at the *meso*-position, is also metabolized to the 3,4- and 10,11-dihydrodiols which formed covalent DNA adducts.[15]

As for DB[*a,c*]A, it is an active tumorigen that formed the 10,11- , 3,4- and the 1,2-dihydrodiols in metabolic studies.[16] Several studies have dealt with the synthesis of these dihydrodiols.[17]

Limited comparative mouse skin assays are available on the methylated DBAs. Whereas introduction of methyl group(s) into the *meso*-position(s) at C-7 and C-14 increased tumorigenicity in the case of DB[*a,h*]A and DB[*a,j*]A (see Fig 2),[8a,18] DB[*a,c*]A and its 9,14-dimethyl-derivative were both found to be weakly active as tumor initiator.[8a] The X-ray

structure of 7,14-dimethyl-DB[*a,j*]A has been determined, showing that methyl introduction at C-7/C-14 causes severe skeletal distortion.[19]

As part of broader study on stable ion study of large methylene-bridged PAHs, low temperature protonation of DB[*a,c*]A and DB[*a,h*]A were included for comparison.[18] In agreement with bromination and nitration, in both cases protonation occurred at the *meso*-region.[20] In the present study we have used a combined experimental NMR and GIAO-DFT study to examine the geometries, relative energies, charge delocalization modes and relative aromaticity in model ring-protonated carbocations derived DB[*a,h*]A and DB[*a,j*]A and their methylated derivatives (compound **1**-**4** and compounds **9**, **11**, and **14** in Fig 2). We have also used DFT to examine the corresponding *anti*-DEs, their ring opening to benzylic carbocations, and covalent adduct formation (quenching) with a model nucleophile.

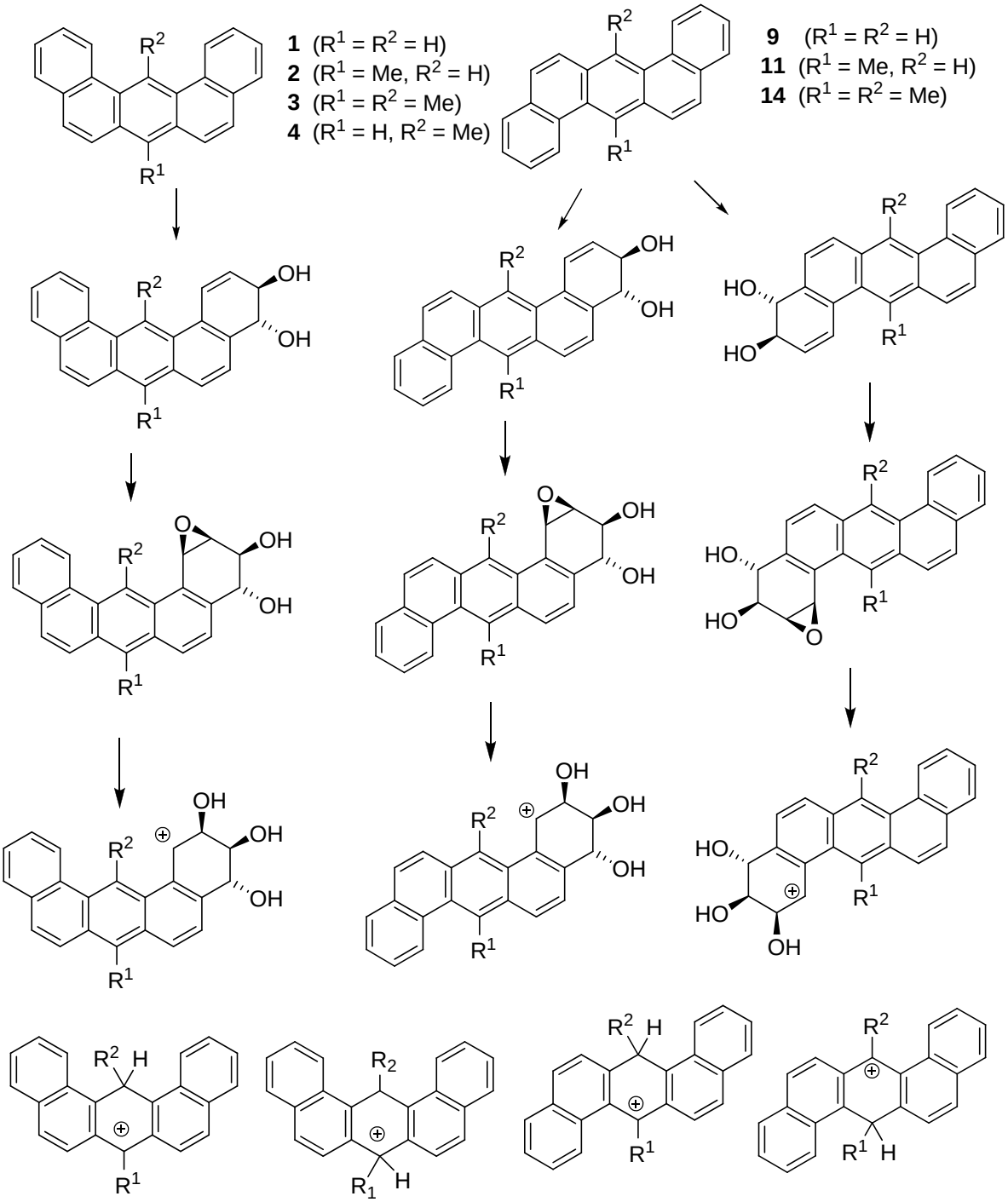

Figure 2. Dibenz [*a*,*j*]anthracenes and dibenz[*a*,*h*]anthracenes, their bay-region dihydrodiols and diol-epoxides metabolites, benzylic carbocations via bay-region epoxide ring opening, and model ring protonated carbocations.

Results and Discussion

Protonation study of dibenz[a,j]anthracene (1) and its methylated derivatives (2-4) (Scheme 1 ; Charts 1-3 and S1; Tables S1-S3; Figures S1-S4).

The ^{1}H and ^{13}C NMR assignments for the neutral dibenzanthracenes **1**, **2**, and **3** are gathered in Chart S1.

Low temperature reaction of parent DB[*a,j*]A **1** with FSO_3H/SO_2ClF gave rather broad NMR signals, likely due to competing oxidation to form the radical cation. Protonation with the less oxidizing CF_3SO_3H/SO_2ClF produced improved NMR spectra, with less signal-broadening (Figure S1), which indicated the formation of carbocations **1aH**$^+$ and **1bH**$^+$ in 1:1 ratio. Based on DFT (Table S1) **1bH**$^+$ is more stable than **1aH**$^+$ by 1.8 kcal/mol.

Protonation of **2** in CF_3SO_3H or in FSO_3H/SO_2ClF gave carbocation **2aH**$^+$ (>95% by NMR) by protonation at C-14 (see Figure S2). DFT computes **2bH**$^+$ to be only 1.6 kcal/mol less stable (Table S1).

Protonation of the carcinogenic dimethyl-derivative **3** in FSO_3H/SO_2ClF gave the carbocation **3aH**$^+$ by *ipso*-attack at C-14 (~95% by NMR; see Figures S3 and S4). Anisotropic shielding of the *ipso* methyl protons in **3aH**$^+$ is noteworthy, appearing at 1.61 ppm (the other methyl is at 3.51 ppm). This shielding effect is analogous to the previously reported examples of *ipso*-protonated methyl- and ethyl-BA carbocations.[9,10] Presence of tiny methyl signals at 3.83 and 1.77 ppm appear consistent with minor formation of **3bH**$^+$ (<5%).

Relief of steric crowding by protonation at C-14 can be inferred from DFT for compound **4** (Table S1), showing **4bH**$^+$ to be 6.3 kcal/mol more stable. Preference for *ipso* attack at C-14 becomes more pronounced in the dimethyl-derivative **3**, where **3aH**$^+$ (observed) is computed to be 9.1 kcal/mol more stable.

Table S2 addresses the angles between various rings from the optimized structures for the DBAs and their protonation carbocations. Whereas parent **1** and its carbocations are planar, methylation at C-7 induces slight deviations (up to 14^o). The situation changes in the C-7/C-14 dimethyl-derivative **3** and its carbocations, where the structure becomes significantly more distorted out of planarity (for example 16^o angle between AC and CE rings in **3**). The correspondence between the reported X-ray structure[20] and the computed gas phase structure seems poor (Table S3)! The *ipso*-protonated carbocations **3aH**$^+$/**3bH**$^+$ remain buckled. Parent **9** is planar but its *meso*-methylated derivatives and their carbocations are severely distorted, with **14** showing an AE angle of 40^o! The degree of bucking diminishes upon *ipso*-protonation (as in **14H**$^+$).

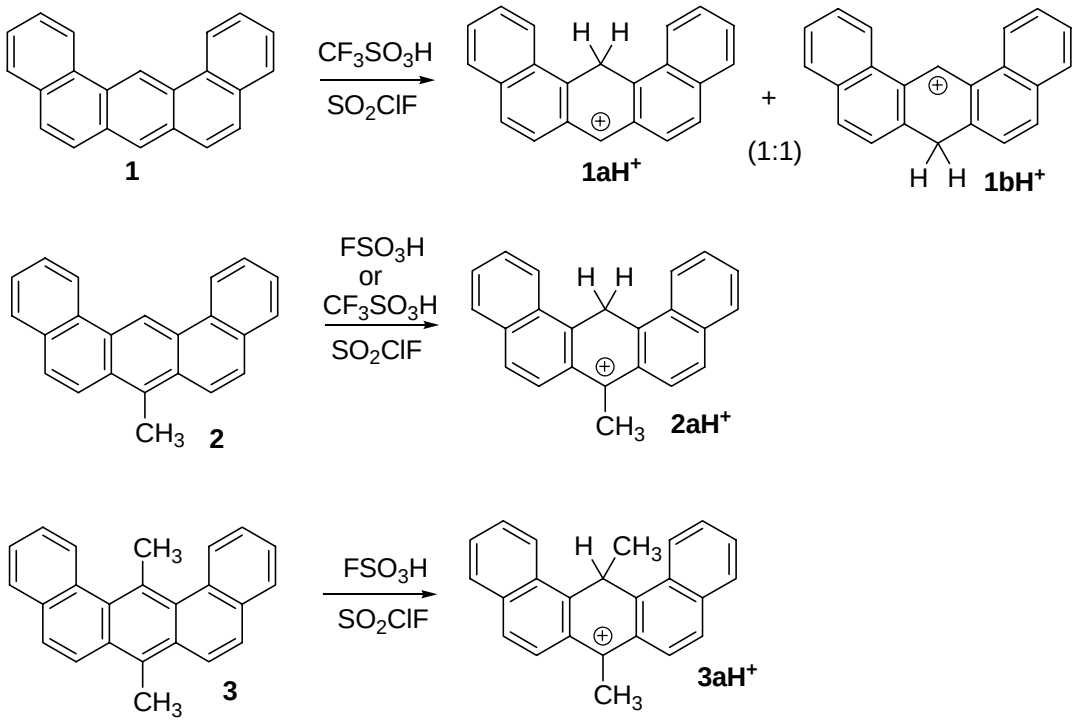

Scheme 1. Protonation of dibenz[*a*,*j*]anthrancenes.

Charts S2-S3 address the relative aromaticity in DBAs **1-4** and their carbocations by using NICS(1)$_{zz}$.[21] There are minor variations in relative aromaticity in the angular rings, with methyl introduction, as distortions forces them out of planarity, so that angular rings become slightly more aromatic. Although NICS(1)$_{zz}$ implies that the *meso*-protonated center rings are no longer aromatic, observation of anisotropic shielding of the *meso*-methyl protons argues that strong ring current effects still operate and the systems are therefore overall aromatic.

The experimental and GIAO-NMR data for the resulting carbocations (at the 6-31G(d) and 6-311+G(d,p) levels), along with their NPA-derived charge delocalization maps are gathered in Charts 1-4 for comparison (for relative energy data see Table S1).

NMR chemical shifts computed at the augmented basis-set are typically circa 10-15 ppm more deshielded and appear to correspond more closely with the available experimental ^{13}C NMR values. Charts 5a and 5b summarize the GIAO-NMR data for the carbocations derived from *meso*-protonation of DB[*a*,*h*]A which were computed at two different basis-sets for comparison (no parallel experimental NMR data could be obtained on this set due to lack of availability of the authentic compounds). The charge delocalization maps derived from $\Delta\delta^{13}$C values correspond closely with those derived based on changes in the NPA-charges (cation minus neutral).

A major difference between the overall charge delocalization modes in the DBA carbocations, as revealed from this work, and the previously studied alkyl-BA carbocations [9,10] is that in the BA carbocations a more distinct anthracenium ion character exists, whereas with DBA

carbocations the delocalization path is less extended and less homogeneous. This could stem from increased twisting of the framework in the DBA carbocations.

DFT Study of the benzylic carbocations via epoxide ring opening (Figure 2, Chart 6; Table S2).
In the context of the present stable ion study and for comparison, the bay-region DEs **5**-**8** derived from DB[*a,j*]A compounds **1**-**4** and the bay-region DEs (**10**, **12**, **13** and **15**) derived from DB[*a,h*]A (compounds **9**, **11**, and **14)**, and their derived carbocations (see further) were computed by DFT. Using a model methanol quenching experiment, relative energies of the *syn* and *anti* methyl ethers were also computed for comparison. Table S4 summarizes the relative energy data.

The NPA-derived charge delocalization maps for the benzylic carbocations $\mathbf{5}^+$ and $\mathbf{10}^+$ derived from the *anti*-DEs of DB[a,j]A **1** and DB[a,h]A **9** were also determined and are sketched in Chart 6, showing that the positive charge is extensively delocalized into the anthracene moiety The 6/7 positions in $\mathbf{5}^+$ and 5/13/14 positions in $\mathbf{10}^+$ (using numbering system in Fig 1) are sites that are potentially susceptible to attack by nucleophile!

Effect of steric congestion in the bay-region on the relative ease of carbocation formation can be deduced by comparing the relative energies of isomeric carbocations $\mathbf{7}^+$ and $\mathbf{6}^+$ (formation of $\mathbf{7}^+$ being more favorable by 1.7 kcal/mol). In the case of $\mathbf{5}^+$, the methoxy-adduct with *anti* stereochemistry is favored by 1.5 kcal/mol. This preference almost vanishes in the case of $\mathbf{7}^+$, for which adducts **7a**/**7b** have nearly the same energies. This is also true in the case of adducts **8a**/**8b** via carbocations $\mathbf{8}^+$. The bay-region carbocations $\mathbf{10}^+$, $\mathbf{12}^+$, $\mathbf{13}^+$, and $\mathbf{15}^+$ (via the *anti*-DEs of DB[*a,h*]A) are more easily formed as compared to carbocations $\mathbf{5}^+$-$\mathbf{7}^+$ (via the *anti*-DEs of DB[*a,j*]A). The computed relative preference for carbocation formation via the DEs in DB[*a,j*]A increases with methyl introduction at C-14 and becomes quite notable with the dimethyl-derivatives (~ 4 kcal/mol) (see Table S4). The preference for *anti* stereochemistry in the adduct formed via **10** is larger than that via **5**, and the same observation is made for **12** versus **6**. Interestingly, whereas relative preference for the *syn* and *anti* adduct formation is diminished in the case of *anti*-DE derived from DB[*a,h*]A by introduction of methyl at C-14, preference for *anti*-stereochemistry increases for the *anti*-DE derived from DB[*a,h*]A (for **7** and **8** the *syn/anti* energy differences are 0.2 and 0.1 kcal/mol respectively, whereas they are 1.6 and 1.3 kcal/mol respectively for **13** and **15**).

The higher tumorigenic potencies of DB[*a,h*]A and in particular the *meso*-methylated derivatives relative to the corresponding DB[*a,j*]A compounds seem to correlate with the present computational data, showing stronger tendencies for carbocation forrmation from the *anti*-DEs in the former group.

Interestingly, whereas *anti/syn* stereoselectivity for covalent adduct formation with methanol (as a model reaction) practically vanishes with increasing steric congestion in DB[*a,j*]A, *anti*-selectivtiy for adduct formation increases with increasing steric crowding for the *anti*-DEs of DB[*a,h*]A.

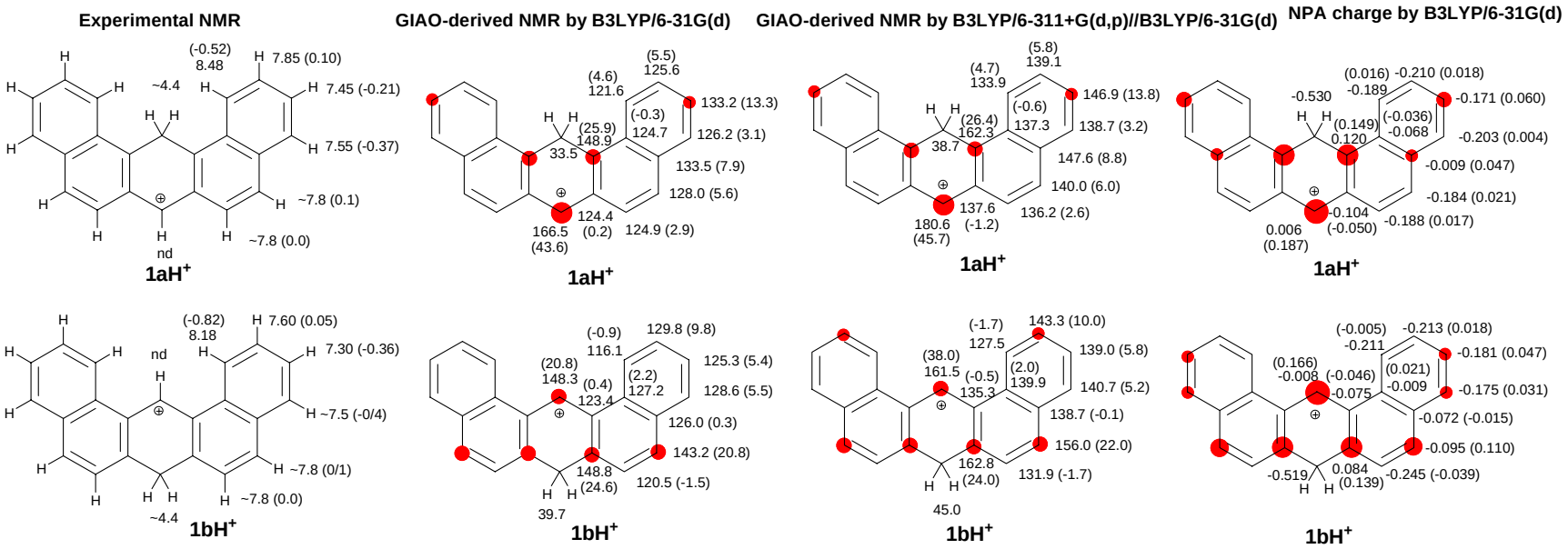

Chart 1. Experimental ^{1}H NMR, GIAO-derived ^{13}C NMR and NPA-derived charges for the carbocations derived from **1** ($\Delta\delta^{13}$C values and NPA change of charges relative to those of the corresponding hydrocarbons in parentheses; a-d denote interchangeable assignments; nd = not determined).

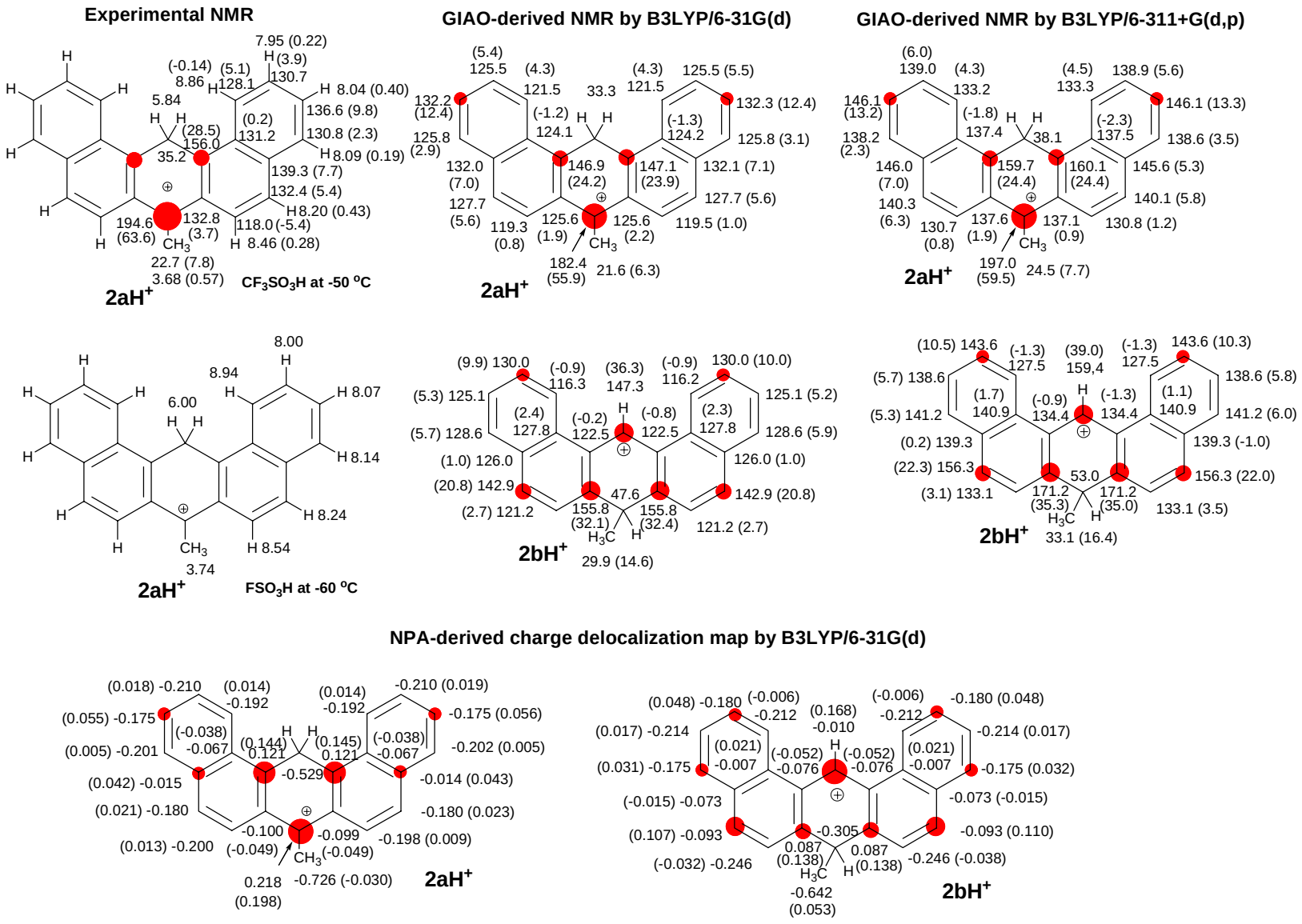

Chart 2. Experimental and GIAO-derived NMR data and computed NPA-derived charges for the carbocations derived from **2** ($\Delta\delta^{13}C$ values and NPA change of charges relative to those of the corresponding hydrocarbons in parentheses).

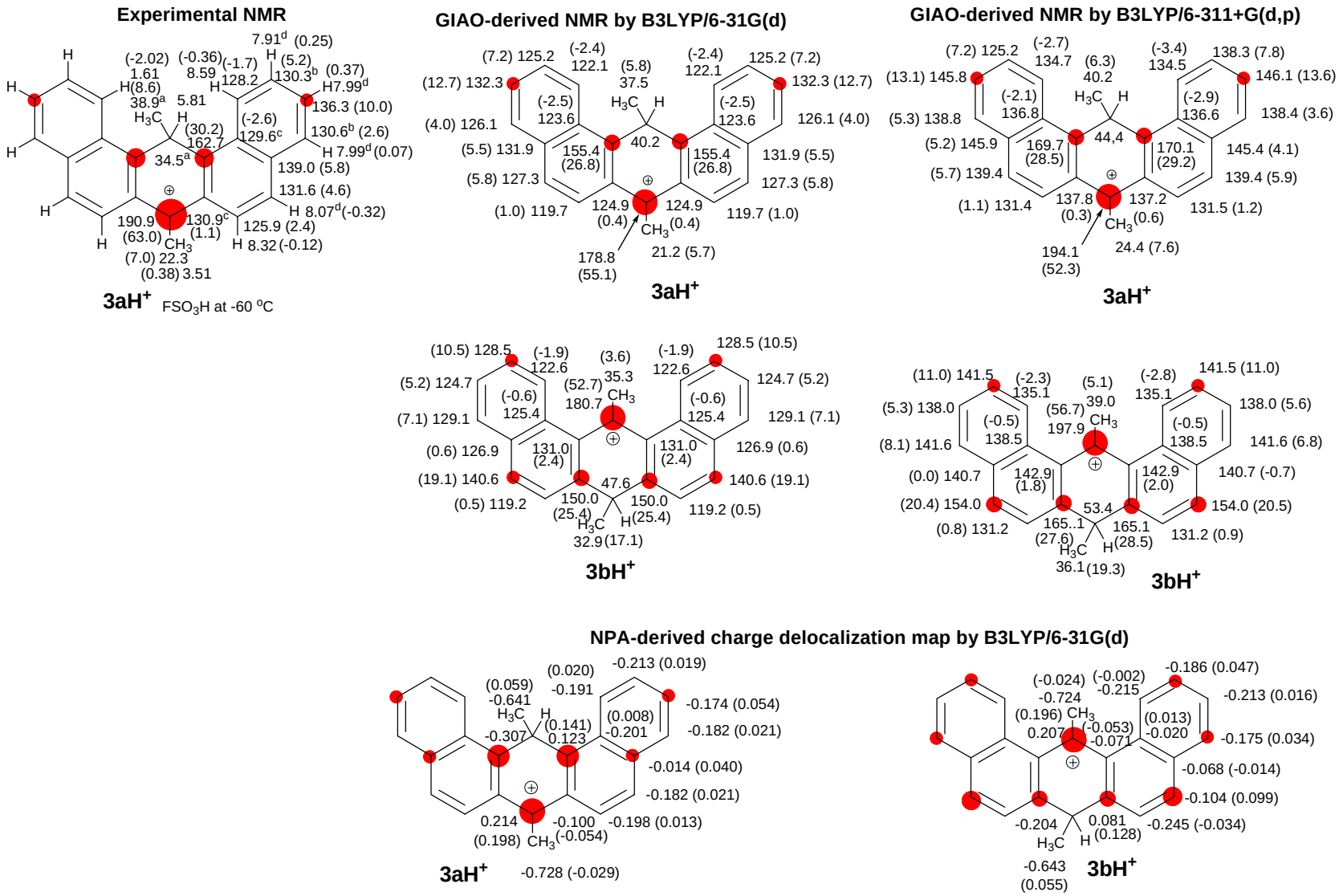

Chart 3. Experimental and GIAO-derived NMR data and computed NPA-derived charges for the carbocations derived from **3** ($\Delta\delta^{13}C$ values and NPA change of charges relative to those of the corresponding hydrocarbons in parentheses).

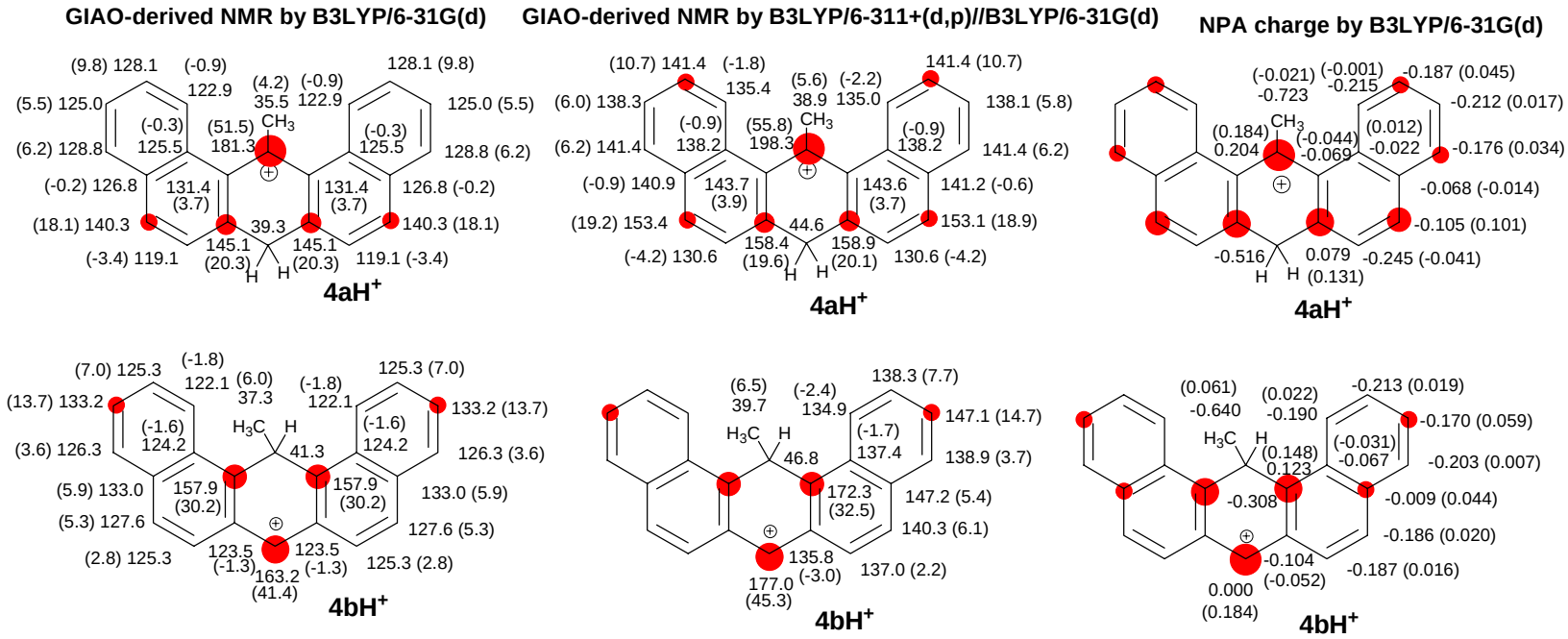

Chart 4. GIAO-derived NMR and computed NPA-derived charges for the carbocations derived from **4** (GIAO $\Delta\delta^{13}$C values and NPA change of charges relative to those of the corresponding hydrocarbons in parentheses).

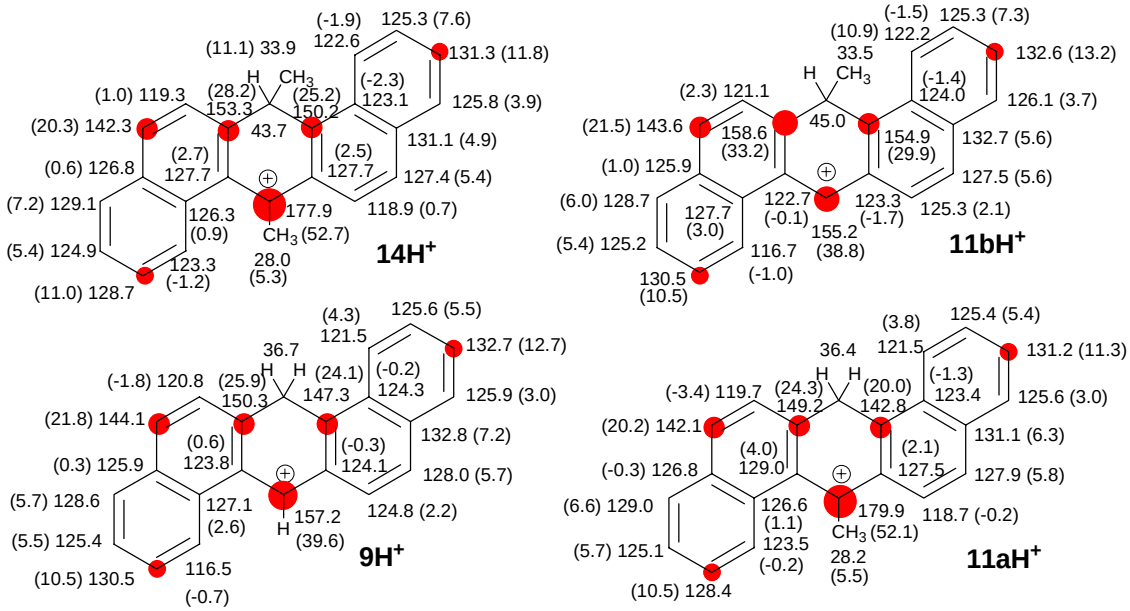

Chart 5a. GIAO-derived NMR data for the carbocations of dibenz[*a*,*h*]anthracenes by B3LYP/6-31G(d) (GIAO $\Delta\delta^{13}$C values relative to those of the corresponding hydrocarbons in parentheses).

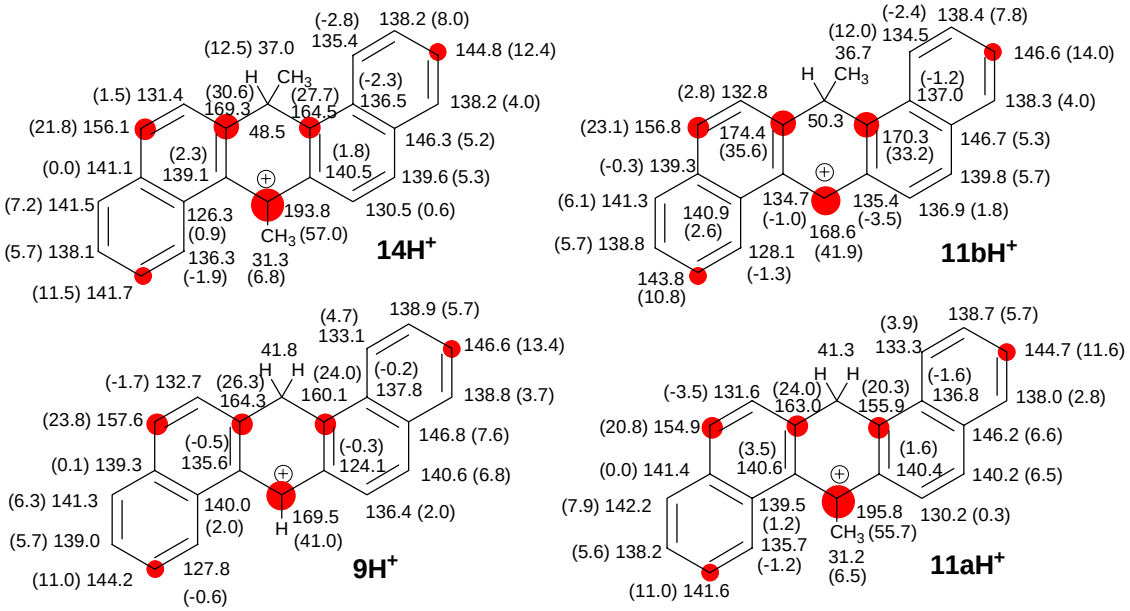

Chart 5b. GIAO-derived NMR data for the carbocations of dibenz[*a*,*h*]anthracenes by B3LYP/6-311+G(d,p)//B3LYP/6-31G(d) (GIAO $\Delta\delta^{13}$C values relative to those of the corresponding hydrocarbons in parentheses).

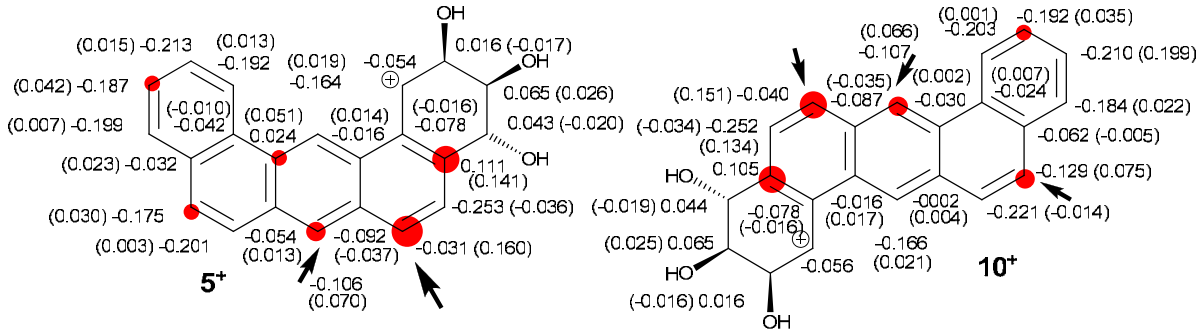

Chart 6. NPA-derived charge delocalization map for the benzylic carbocations $\mathbf{5}^+$ and $\mathbf{10}^+$ via *anti* diol-epoxides **5** and **10** by B3LYP/6-31G(d) (changes of charges relative to the corresponding diol-epoxides in parentheses; Arrows identify positions of highest positive charge that could potentially be target for attack by nucleophile).

Experimental Section

General Procedures. The ^{1}H and ^{13}C NMR spectra of the neutral substrates were recorded on a 400 MHz instrument. Low temperature NMR studies of the carbocations were performed on a 500 MHz instrument at the specified temperatures.
FSO_3H and CF_3SO_3H were freshly distilled twice in all-glass apparatus under inert atmosphere of nitrogen. SO_2ClF was prepared according to a modified procedure of Prakash et al.[22] Compounds (**1**)[23,24] and the methyl-derivatives (**2**[24] and **3**[25]) were small gift samples, kindly donated by Prof. R. G. Harvey (Univ of Chicago Ben May Institute).

Carbocation generation in FSO_3H or CF_3SO_3H/SO_2ClF. The substrate (5-10 mg) was placed in a 5 mm NMR tube. Into the NMR tube, which was cooled in a dry-ice acetone bath (-78 ºC), SO_2ClF (0.5 ml) was condensed. FSO_3H or CF_3SO_3H (2-3 drops) was then added under a nitrogen atmosphere at dry ice-acetone temperature. The resulting colored solution was efficiently mixed (vortex mixer). Finally a few drops (2-3 drops) of cold CD_2Cl_2 were added to the NMR tube. The resulting solution was once again mixed (vortex) prior to NMR study. The color of the studied carbocation solutions were dark-red except for **1** in CF_3SO_3H/SO_2ClF (dark-blue).

Quenching experiments. Cold solutions of the carbocations in NMR tubes were poured into ice-sodium bicarbonate. The resulting mixture was extracted with CH_2Cl_2 and dried ($MgSO_4$). After evaporation of the solvent, the residue was analyzed by ^{1}H NMR, which confirmed the recovery of skeletally intact PAHs in all cases.

Computational protocols. Structures were optimized using a C_1 molecular point group by the density function theory (DFT) method at B3LYP/6-31G(d) level using the Gaussian 03 package.[26,27] All computed geometries were verified by frequency calculations to have no imaginary frequencies. Energies are summarized in Tables S1 and S4. Natural population analysis (NPA)-derived charges were computed at the same level. NMR chemical shifts were calculated by the GIAO[28] method at the B3LYP/6-311+G(d,p)//B3LYP/6-31G(d) and B3LYP/6-31G(d)//B3LYP/6-31G(d) level. NMR chemical shifts were referenced to TMS (GIAO magnetic shielding tensor = 184.1 and 189.8 ppm in TMS; these values are related to the GIAO isotropic magnetic susceptibility for ^{13}C), calculated with molecular symmetry of T_d at the same level of theory. Nuclear independent chemical shifts (NICS)[29] were calculaued by the GIAO method by B3LYP/6-311+G(d,p)//B3LYP/6-31G(d). The "out-of-plane" components of the NICS tensors were calculated at 1 Å above the ring centers by rotation the planes of the rings orthogonal to *z*-axis, which denotes as $NICS(1)_{zz}$.[30] The ring centers were defined as the simple average of Cartesian coordinates for all the carbons in the ring. Planes of the rings were calculated by least-square methods using coordinates of the all carbons in the rings.

Supplementary Information Available

Chart S1 (NMR assignments for 1-3); Charts S2-S3 (NICS data); Tables S1 and S4 (energy data); Tables S2-S3 (angles between rings); Figures S1-S4 (selected NMR spectra for the carbocations).

Acknowledgements

This work was partially supported by the NCI of NIH (2R15CA078235-02A1).

References

1. Harvey, R. G. *Polycyclic Aromatic Hydrocarbons; Chemistry and Carcinogenicity*; Cambridge Monographs on Cancer Research, Cambridge University Press: Cambridge, UK, 1991
2. Wislocki, P. G.; Lu, A. Y. H. In *Polycyclic Aromatic Hydrocarbon Carcinogenesis: Structure-Activity Relationships*, Yang, S. K.; Silverman, B. D. Eds., CRC Press: Boca Raton, Florida, 1988; Vol. 1, Ch. 1.
3. Jerina, D. M.; Sayer, J. M.; Agrawal, S. K.; Yagi, H.; Levin, W.; Wood, A. W.; Conney, A. H.; Pruess-Schwatz, D.; Baird, W. M.; Pigott, M. A.; Dipple, A. In *Biological Reactive Intermediates III*, Kocsis, J. J.; Jollow, D. J.; Witmer, C. M.; Nelson, J. O.; Snyder, R. Eds.; Plenum Press, New York, 1986; pp 11-30.
4. Szeliga, J.; Dipple, A. *Chem. Res. Toxicol*. **1998**, *11*, 1.
5. Geacintov, N. E. In *Polycyclic Aromatic Hydrocarbon Carcinogenesis: Structure-Activity Relationships*, Yang, S. K.; Silverman, B. D. Eds., CRC Press: Boca Raton, Florida, 1988; Ch. 7, Vol. 2.
6. Laali, K. K. In *Carbocation Chemistry*, Olah, G. A.; Prakash, G. K. S. Eds., Wiley: New York, 2004; Ch. 9.
7. (a) Krzeminski, J.; Lin, J-M.; Hecht, S. H. *Chem. Res. Toxicol*. **1994**, *7*, 125. (b) Giles, A. S.; Seidel, A.; Philips, D. H. *Chem. Res. Toxicol*. **1997**, *10*, 1275. (c) Kiselyov, A. S.; Lee, H.; Harvey, R. G. *J. Org. Chem*. **1995**, *60*, 6123. (d) Sharma, A. K.; Amin, S. *Chem. Res. Toxicol*. **2005**, *18*, 1438. (e) Sharma, A. K.; Lin, J.-M.; Desai, D.; Amin, S. *J. Org. Chem*. **2005**, *70*, 4962. (f) Lakshman, M. K.; Kole, P. L.; Chaturvedi, S.; Saugier, J. H.; Yeh, H. J. C.; Glusker, J. P.; Carrell, H. L.; Katz, A. K.; Afshar, C. E.; Dashwood, W.-M.; Kenniston, G.; Baird, W. M. *J. Am. Chem. Soc*. **2000**, *122*, 12629.
8. (a) Hecht, S. S.; Melikian, A. A.; Amin, S. In *Polycyclic Aromatic Hydrocarbon Carcinogenesis: Structure-Activity Relationships*, Yang, S. K.; Silverman, B. D. Eds, CRC Press: Boca Raton, Florida, 1988; Vol. 1, Ch. 4. (b) Hecht, S. S.; Melikian, A. A.; Amin, S.

Acc. Chem. Res. **1986**, *19*, 174. Yang, S. K. In *Polycyclic Aromatic Hydrocarbon Carcinogenesis: Structure-Activity Relationships*, Yang, S. K.; Silverman, B. D. Eds, CRC Press: Boca Raton, Florida, 1988; Vol. 1, Ch. 5.
9. Laali, K. K.; Arrica, M. A.; Okazaki, T.; Harvey, R. G. *J. Org. Chem*. **2007**, *72*, 6768.
10. Laali, K. K.; Tanaka, M. *J. Org. Chem*. **1998**, *63*, 7280.
11. Boyd, D. R.; O'Kane, G. A. *J. Chem. Soc. Perkin Trans 1*, **1990**, 2079.
12. Chadha, A.; Sayer, J. M.; Yeh, H. J. C.; Yagi, H.; Cheh, A. M,; Pannell, L. K.; Jerina, D. M., *J. Am. Chem. Soc*. **1989**, *111*, 5456.
13. (a) Harvey, R. G.; Dai, W.; Zhang, J.-T.; Cortez, C., *J. Org. Chem*. **1998**, *63*, 8118. (b) Zhang, J.-T.; Dai, W.; Harvey, R. G., *J. Org. Chem*. **1998**, *63*, 8125.
14. Nordqvist, M.; Thakker, D. R.; Levin, W.; Yagi, H.; Ryan, D. E.; Thomas, P. E.; Conney, A. H.; Jerina, D. M. *Mol. Pharmacol*. **1979**, *16*, 643.
15. Fu, P. P.; Von Tungeln, L. S.; Chiu, L.-H.; Zhan, D.-J.; Deck, J.; Bucci, T.; Wang, J.-C., *Chem. Res. Toxicol*. **1998**, *11*, 937.
16. Lecoq, S.; Perin, F.; Plessis, M. J.; Duquesne, M. *Carcinogenesis* **1989**, *10*, 461.
17. (a) Harvey, R. G.; Fu, P. P. *J. Org. Chem*. **1980**, *45*, 169. (b) Kole, P. L.; Dubey, S. K.; Kumar, S. *J. Org. Chem*. **1989**, *54*, 845. (c) Kumar, S.; Kole, P. L. *Tetrahedron Lett*. **1987**, *28*, 4363. (d) Kole, P. L.; Kumar, S. *J. Chem. Soc., Perkin Trans.1* **1991**, 2151.
18. Laali, K. K.; Okazaki, T.; Harvey, R. G. *J. Org. Chem*. **2001**, *66*, 3977.
19. Harvey, R. G.; Cortez, C.; Sawyer, T. W.; DiGiovanni, J. *J. Med. Chem*. **1988**, *31*, 1308.
20. Carrell, C. J.; Carrell, H. L.; Glusker, J.; Abu-Shaqara, E.; Cortez, C.; Harvey, R. G. *Carcinogenesis* **1994**, *15*, 2931.
21. Milles, N. S.; Liagostera, K. *J. Org. Chem.* **2007**, *72*, 9163 and related references cited therein.
22. Reddy, V. P.; Bellew, D. R.; Prakash, G. K. S. *J. Fluorine Chem.* **1992**, *56*, 195.
23. Harvey, R. G.; Pataki, J.; Cortez, C.; Di Raddo, P.; Yang, C. X. *J. Org. Chem.* **1991**, *56*, 1210.
24. Harvey, R. G.; Cortez, C.; Jacobs, S. A. *J. Org. Chem.* **1982**, *47*, 2120.
25. Martin, R. H. *Bull. Soc. Chim. Belg.* **1949**, *58*, 87.
26. Koch, W.; Holthausen, M. C. *A Chemist's Guide to Density Functional Theory*; 2nd Ed., Wiley-VCH: Weinheim, 2000.
27. Frisch, M. J.; Trucks, G. W.; Schlegel, H. B.; Scuseria, G. E.; Robb, M. A.; Cheeseman, J. R.; Montgomery, J. A., Jr.; Vreven, T.; Kudin, K. N.; Burant, J. C.; Millam, J. M.; Iyengar, S. S.; Tomasi, J.; Barone, V.; Mennucci, B.; Cossi, M.; Scalmani, G.; Rega, N.; Petersson, G. A.; Nakatsuji, H.; Hada, M.; Ehara, M.; Toyota, K.; Fukuda, R.; Hasegawa, J.; Ishida, M.; Nakajima, T.; Honda, Y.; Kitao, O.; Nakai, H.; Klene, M.; Li, X.; Knox, J. E.; Hratchian, H. P.; Cross, J. B.; Adamo, C.; Jaramillo, J.; Gomperts, R.; Stratmann, R. E.; Yazyev, O.; Austin, A. J.; Cammi, R.; Pomelli, C.; Ochterski, J. W.; Ayala, P. Y.; Morokuma, K.; Voth, G. A.; Salvador, P.; Dannenberg, J. J.; Zakrzewski, V. G.; Dapprich, S.; Daniels, A. D.; Strain, M. C.; Farkas, O.; Malick, D. K.; Rabuck, A. D.; Raghavachari, K.; Foresman, J. B.;

Ortiz, J. V.; Cui, Q.; Baboul, A. G.; Clifford, S.; Cioslowski, J.; Stefanov, B. B.; Liu, G.; Liashenko, A.; Piskorz, P.; Komaromi, I.; Martin, R. L.; Fox, D. J.; Keith, T.; Al-Laham, M. A.; Peng, C. Y.; Nanayakkara, A.; Challacombe, M.; Gill, P. M. W.; Johnson, B.; Chen, W.; Wong, M. W.; Gonzalez, C.; Pople, J. A. *Gaussian 03*, Revision B.05; Gaussian, Inc.: Pittsburgh, PA, 2003.

28. (a) Wolinski, K.; Hinton, J. F.; Pulay, P. *J. Am. Chem. Soc.* **1990**, *112*, 8251. (b) Ditchfield, R. *Mol. Phys.* **1974**, *27*, 789.
29. Schleyer; P. v. R.; Maerker, C.; Dransfeld, A.; Jiao, H.; Eikema Hommes, N. J. R. *J. Am. Chem. Soc.* **1996**, *118*, 6317.
30. Corminboeuf, C.; Heine, T.; Seifert, G.; Schleyer, P.v. R.; Weber, J. *Phys. Chem., Chem. Phys.* **2004**, *6*, 273.